Available online at www.sciencedirect.com
ScienceDirect
Cement and Concrete Research 36 (2006) 1879–1885
Cement and Concrete Research

Model of piezoresistivity in carbon fiber cement

Sihai Wen, D.D.L. Chung *

Composite Materials Research Laboratory, University at Buffalo, State University of New York, Buffalo, NY 14260-4400, USA

Received 17 June 2004; accepted 24 March 2006

Abstract

Piezoresistivity in carbon fiber cement allows strain sensing. It was first reported in 1993, but this paper provides the first theoretical model for this phenomenon. The model is based on the concept that the piezoresistivity is due to the slight pull-out of crack-bridging fibers during crack opening and the consequent increase in the contact electrical resistivity of the fiber–matrix interface. Good agreement is found between theory and experimental results obtained under tension/compression.

Keywords: Electrical properties; Cement paste; Strain effect; Microcracking; Piezoresistivity

1. Introduction

Carbon fiber cement–matrix composites are structural materials that are gaining in importance quite rapidly due to the decrease in carbon fiber cost and the increasing demand of superior structural and functional properties. These composites contain short carbon fibers, typically 5 mm in length, as the short fibers can be used as an admixture in concrete (whereas continuous fibers cannot be simply added to the concrete mix) and short fibers are less expensive than continuous fibers.

Although carbon fibers help the structural performance of cement-based materials, they are most valuable in improving the functional properties, particularly the ability to sense strain rendered by carbon fiber addition pertaining to the strain sensing ability [1–14].

Although there are considerable experimental results on the piezoresistivity of carbon fiber cement [15], theoretical understanding of the phenomena is limited to a plausible mechanism involving slight fiber pull-out upon crack opening and the consequent loosening of the fiber–matrix interface and increase in the contact electrical resistivity of this interface [9,16]. This paper provides the first model of the phenomenon.

2. Modelling[1]

Consider a carbon fiber reinforced cement specimen in the shape of a parallelepiped, such that the part of the specimen for which the resistance is measured (i.e., the part between the voltage electrical contacts in the four-probe method of electrical resistance measurement) is of size $L \times W \times H$. The specimen is under tensile stress σ in the elastic regime and the crack is parallel to the front rectangular surface of the specimen (Fig. 1). The cross-section of the crack is in the shape of an ellipse with dimensions $2a$ and $2b$ in the major and minor axes respectively. The crack width is t in the direction into the paper in Fig. 1. Let the angle between the minor axis and the stress direction be θ. In order to determine the force F_c applied on the crack (Fig. 2), project the crack on the bottom rectangular surface of the rectangular parallelepiped. The projected area A_p of crack is expressed by the equation

$$A_p = L_p t, \tag{1}$$

where L_p is the projected length of major axis of crack (i.e., $2a \cos \theta$). Therefore,

$$A_p = 2at \cos \theta. \tag{2}$$

The force F_c is given by

$$F_c = A_p \sigma. \tag{3}$$

* Corresponding author. Tel.: +1 716 645 2593x2243; fax: +1 716 645 3875.
E-mail address: ddlchung@buffalo.edu (D.D.L. Chung).

0008-8846/$ - see front matter © 2006 Elsevier Ltd. All rights reserved.
doi:10.1016/j.cemconres.2006.03.029

[1] The Appendix contains a glossary of symbols used in the theory below.

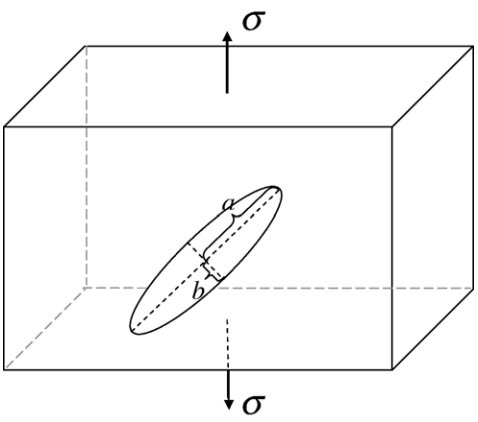

Fig. 1. A crack with the cross-sectional shape of an ellipse has the cross-section parallel to the front surface of a specimen under tension.

Substituting Eq. (2) into Eq. (3), we obtain the equation

$$F_c = 2at\sigma \cos\theta. \quad (4)$$

Let us decompose F_c into two components F_i and F_j, where F_i and F_j are forces for crack closing and opening respectively (Fig. 2). Hence,

$$F_i = F_c \sin\theta = 2at\sigma \sin\theta \cos\theta = at\sigma \sin 2\theta \quad (5)$$

and

$$F_j = F_c \cos\theta = 2at\sigma \cos^2\theta = at\sigma(1+\cos 2\theta) \quad (6)$$

Let us assume that a single fiber (diameter d=15 μm, length L_f=0.5 cm and electrical resistivity $\rho_f = 3.0\times10^{-3}$ Ω. cm, were used in prior experimental work [1–10,17]) bridges the crack with length h embedded in the cement matrix on either side of the crack (Fig. 3). The applied tensile stress σ results in a shear stress τ along the interface between the fiber and the cement matrix. The relationship of F_j with τ is

$$F_j = A_c \tau = 2\pi dh\tau, \quad (7)$$

where A_c is contact area between the fiber and matrix and is equal to $\pi d(2h)$.From Eqs. (6) and (7), we obtain

$$\tau = at\sigma(1+\cos 2\theta)/(2\pi dh). \quad (8)$$

Let the volume fraction of fibers in the rectangular parallelepiped specimen be γ. Then, the total number of fibers (N) contained in the measured part of the specimen is

$$N = \gamma V_s/V_f, \quad (9)$$

where V_s=LWH is the volume of the measured part of the specimen and V_f is the volume of an individual fiber.

$$V_f = \pi d^2 L_f/4 \quad (10)$$

Then Eq. (9) becomes

$$N = 4\gamma\, LWH/(\pi d^2 L_f) \quad (11)$$

Let us divide the parallelepiped into N rectangular parallelepiped unit cells of dimensions M, Q and S (Fig. 4(a)). Since there are a total of N fibers, there is one fiber per unit cell. The resistance of a

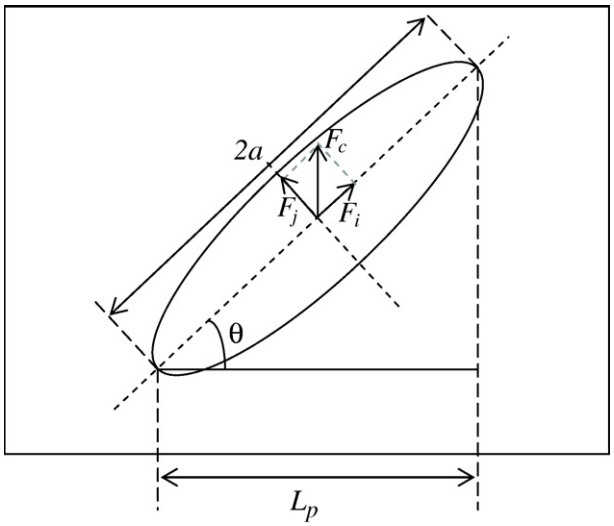

Fig. 2. The force F_c applied to the crack is decomposed into two components F_i and F_j along the major and minor axes of the crack respectively.

unit cell in the direction of the fiber is contributed by (i) conduction paths within the cement matrix surrounding a crack with the bridging fiber and (ii) the bridging fiber itself. The matrix portion of the unit cell is divided into three parts that are marked A, B and C (Fig. 4(b)). Let the volume resistance contributions by A, B, C and the fiber be R_A, R_B, R_C and R_v respectively. If R_v is much smaller than R_B, the crack-bridging fiber dominates the electrical conduction between A and C and the resistors R_A, R_v and R_C are in series. If R_v is not much smaller than R_B, the resistors R_v and R_B are in parallel.

$$R_v = \rho_f L_f/A_f = \rho_f L_f/(\pi d^2/4), \quad (12)$$

where A_f is the cross-sectional area of the fiber.

$$R_B = \rho_m L_m/A_m, \quad (13)$$

where ρ_m is volume resistivity of the matrix, i.e., 4.87×10^5 Ω cm [18], L_m is the length of B (Fig. 4(b)) and A_m is the cross-sectional area of B.

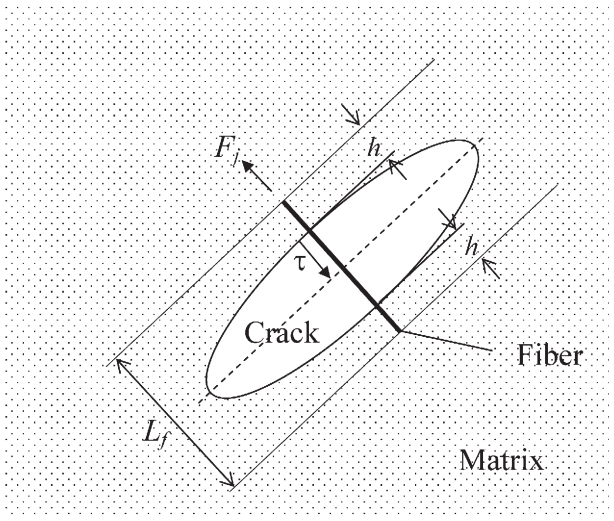

Fig. 3. A single carbon fiber bridging a crack is along the minor axis of the crack. The fiber is embedded in the cement matrix with length h on either side of the crack.

The unit cell volume V_u is given by

$$V_u = MQS = V_s/N, \tag{14}$$

Let us approximate S as L_f (Fig. 4(b)). From Eqs. (14) and (11),

$$MQ = \pi d^2/4\gamma. \tag{15}$$

The maximum value of A_m is MQ (Fig. 4(c)). From Eq. (13),

$$R_B > \rho_m L_m/(MQ) = 4\ \gamma\rho_m L_m/(\pi d^2) \tag{16}$$

Substituting $\rho_f = 3.0\times10^{-3}$ Ω. cm, $L_f = 0.5$ cm, $d = 1.5\times10^{-3}$ cm, $\rho_m = 4.87\times10^5$ Ω. cm, $L_m = 1.0\times10^{-4}$ cm [15] and $\gamma = 0.48\%$ into Eqs. (12) and (16) yields

$$R_v = 8.49\times10^2\Omega \tag{17}$$

and

$$R_B > 1.32\times10^5\Omega. \tag{18}$$

Hence, R_B is much greater than that of R_v. Therefore, R_A, R_v and R_C are in series.

The interface between fiber and matrix is associated with a contact resistance R_i. To include R_i in the theory, the overall resistance R_f of a fiber can be considered to be equal to the sum of the volume resistance R_v and the contact resistance R_i, i.e.,

$$R_f = R_v + R_i. \tag{19}$$

The equivalent circuit is shown in Fig. 4(d). Hence, the total resistance is

$$R = R_A + R_v + R_i + R_C. \tag{20}$$

Since the dimensions of A and B and the fiber are essentially the same, whether the specimen is loaded or not, we can assume R_A, R_C and R_v to be constant. Taking the differential change on both sides of Eq. (19), we obtain

$$\Delta R = \Delta R_i. \tag{21}$$

R_i is defined as

$$R_i = \rho_c/A_c, \tag{22}$$

where ρ_c is the contact electrical resistivity and takes the value of 10^5 Ω. cm^2 [16].Using Eq. (22) and the fact that $A_c = \pi d(2h)$, we obtain

$$R_i = \rho_c/(2\pi dh) \tag{23}$$

Single fiber pull-out testing showed that the contact resistivity gradually increased with increasing shear stress prior to the abrupt

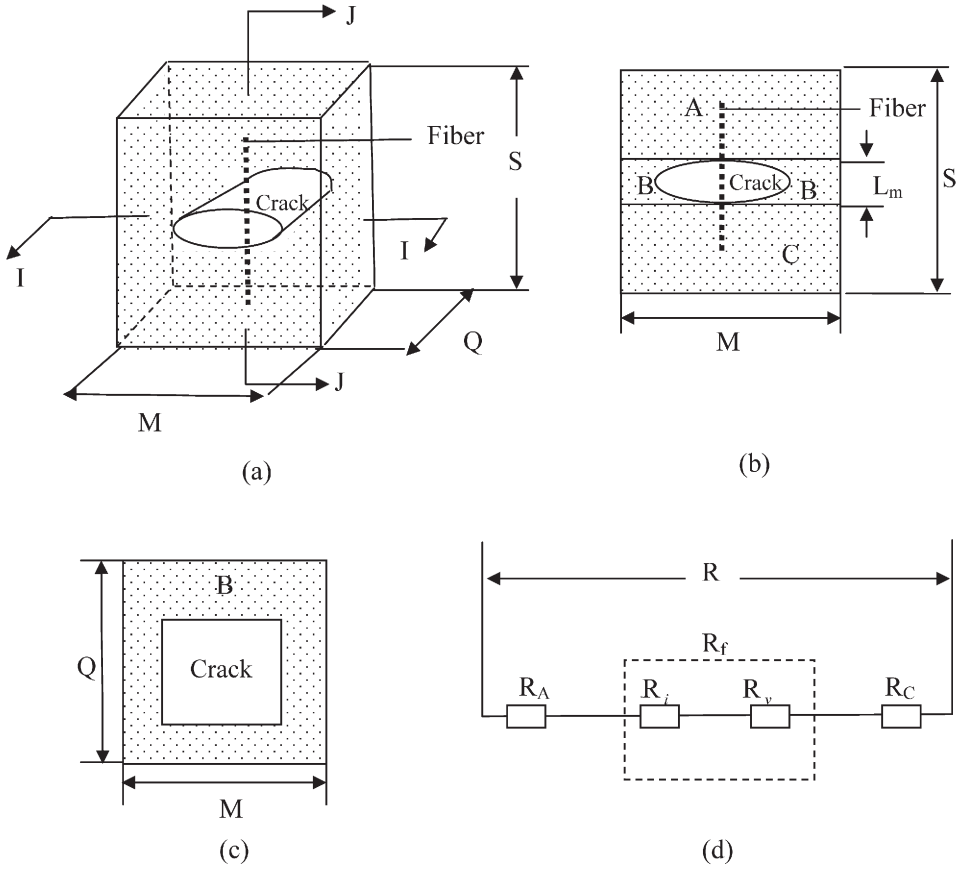

Fig. 4. (a) Three-dimensional schematic illustration of a parallelepiped unit cell of size $M \times Q \times S$ and containing a single fiber (dotted vertical line) that bridges a crack (white region) in the horizontal plane. The cement matrix is the shaded region. (b) J–J section view of the unit cell. (c) I–I section view of the unit cell. (d) Equivalent electrical circuit of the unit cell, showing resistors in series.

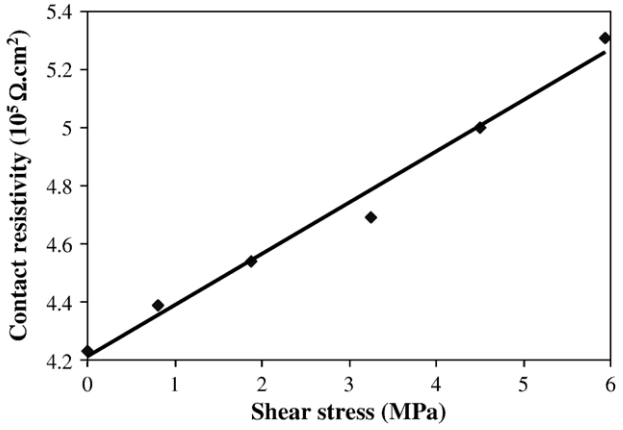

Fig. 5. Curve of contact resistivity versus shear stress for carbon–fiber silica–fume cement paste, based on Fig. 2 of Ref. 16.

increase when the shear stress had reached its maximum [16]. Furthermore, the resistance increased almost linearly with the shear stress τ [16]. This stress may loosen the bond between fiber and cement matrix. Thus,

$$\Delta R = c\Delta\tau = c\Delta[at\sigma(1+\cos 2\theta)/(2\pi dh)] = cat/(2\pi dh)\Delta[\sigma(1+\cos 2\theta)], \quad (24)$$

where c is a proportionality constant.

We shall next determine the constant c in Eq. (24). Based on the data of Fu and Chung [16], we obtain the curve of contact resistivity versus shear stress (Fig. 5). The slope k of this curve is

$$k = 0.1764 \times 10^5\ \Omega.\ \mathrm{cm}^2/\mathrm{MPa} = 1.764 \times 10^{-6}\ \Omega.\ \mathrm{m}^2/\mathrm{Pa}. \quad (25)$$

Using Eqs. (23) and (24), we have

$$\Delta\rho_c = 2\pi dhc\Delta\tau = k\Delta\tau.$$

Thus,

$$c = k/(2\pi dh) = 8.82 \times 10^{-7}/(\pi dh)\Omega.\ \mathrm{m}^2/\mathrm{Pa}. \quad (26)$$

Substituting the value of c into Eq. (24), we obtain

$$\Delta R = (4.41 \times 10^{-7})at/(\pi^2 d^2 h^2)\Delta[\sigma(1+\cos 2\theta)] \quad (27)$$

Since the angle θ between forces F_c and F_j can take values in the range from 0 to $\pi/2$, we can integrate the right side of Eq. (27) with respect to the angle θ ranging from 0 to $\pi/2$ and take the average value over θ. In this way, we obtain the average effect of an individual fiber on the change in resistance of the specimen, i.e.,

$$\Delta R = 1/(\pi/2)\left|\int_0^{\pi/2}(4.41\times10^{-7})at/(\pi^2d^2h^2)\Delta[\sigma(1+\cos 2\theta)]\right| = 1/(\pi/2)\left|(4.41\times10^{-7})at/(\pi^2d^2h^2LW)\sigma[\theta-(\sin 2\theta)/2]\right|_0^{\pi/2} = (4.41\times10^{-7})at\sigma/(\pi^2d^2h^2). \quad (28)$$

In Eq. (28), ΔR is the change in resistance in the loading direction and it is independent of θ.

There are a total of N fibers in the rectangular parallelepiped specimen. Under the condition of uniform fiber distribution, it can be considered that the ends of all fibers (one end of every fiber being considered as representing the position of the fiber) are uniformly distributed, with every fiber end located at the center of a small cube of volume V_u. Here, the small cube is a special case of a rectangular parallelepiped unit cell of dimensions M, Q and S that are all equal (Fig. 4(a)). The distance δ between the ends of two adjacent fibers is the length of an edge of the small cube, that is

$$\delta = \sqrt[3]{V_u} = \sqrt[3]{V_s/N} = \sqrt[3]{LWH/N} \quad (29)$$

Then, in a three-dimensional space of size $L\times W\times H$ we have

$$N_x = L/\delta$$

$$N_y = W/\delta$$

and

$$N_z = H/\delta, \quad (30)$$

where, N_x, N_y and N_z are the number of fiber ends along the x, y and z axes respectively (Fig. 6).

Combining Eqs. (29) and (30), we obtain

$$N_x = \sqrt[3]{NL^2/(WH)}, \quad (31)$$

$$N_y = \sqrt[3]{NW^2/(LH)} \quad (32)$$

and

$$N_z = \sqrt[3]{NH^2/(LW)}. \quad (33)$$

The three-dimensional space of size $L\times W\times H$ (Fig. 6) can be divided into N_z vertical slices of thickness δ. There are N_xN_y fiber ends per slice. Each slice can be divided into N_x columns of width δ. Let the change in resistance of a column, a slice, and the entire $L\times W\times H$ volume be ΔR^V, ΔR^{2D} and ΔR_y^{3D} respectively.

Assume that the fibers in Fig. 6 are all parallel to the y-axis. The assumption of the fibers being parallel to one another is justified by the fact that the average effect of a single fiber on the change in resistance ΔR is independent of the fiber orientation

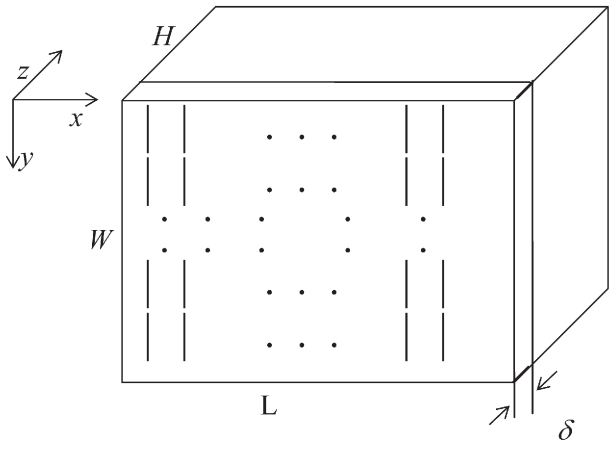

Fig. 6. Distribution of fiber ends in a three-dimensional volume of size $L\times W\times H$. There are N_x, N_y and N_z fiber ends in x, y and z axes respectively.

Table 1
Different combinations of a (half of the length of a crack) and t (thickness of the crack) corresponding to at=50.5 μm^2 and 61.3 μm^2 for the cases of uniaxial compression and uniaxial tension respectively

Row number	t (μm)	a (μm)	
		Compression	Tension
1	10^3	5.05×10^{-2}	6.13×10^{-2}
2	10^2	5.05×10^{-1}	6.13×10^{-1}
3	10	5.05	6.13
4	1.0	5.05×10^{1}	6.13×10^{1}
5	10^{-1}	5.05×10^{2}	6.13×10^{2}
6	10^{-2}	5.05×10^{3}	6.13×10^{3}

(Eq. (28)). Hence, the fibers in a column are electrically in series and all of the N_x columns in a slice and all of the N_z slices are electrically in parallel. Assuming that every fiber contributes equally to the change in resistance, we have

$$\Delta R^V = N_y \Delta R, \tag{34}$$

$$1/\Delta R^{2D} = \sum_i^{N_x} (1/\Delta R_i^V) = N_x/\Delta R^V \tag{35}$$

and

$$1/\Delta R_y^{3D} = \sum_i^{N_z} (1/\Delta R_i^{2D}) = N_z/\Delta R^{2D}. \tag{36}$$

Combining Eqs. (34)–(36), we obtain

$$\Delta R_y^{3D} = N_y \Delta R/(N_x N_z) \tag{37}$$

Substituting Eqs. (31)–(33) into Eq. (37), we obtain

$$\Delta R_y^{3D} = \sqrt[3]{W^4/(L^2H^2N)}\Delta R. \tag{38}$$

Substitution of Eqs. (11) and (28) into Eq. (38) yields

$$\begin{aligned}\Delta R_y^{3D} &= (4.41\times10^{-7})at\sigma/(\pi^2d^2h^2)\sqrt[3]{\pi d^2 L_f W^3/(4\gamma L^3 H^3)} \\ &= (4.41\times10^{-7})\sqrt[3]{L_f/(4\gamma\pi^5 d^4)}(at\sigma/h^2)W/(LH)\end{aligned} \tag{39}$$

Similarly, if all the fibers are parallel to the x and z axes, we can derive the following two equations respectively:

$$\Delta R_x^{3D} = (4.41\times10^{-7})\sqrt[3]{L_f/(4\gamma\pi^5 d^4)}(at\sigma/h^2)L/(WH) \tag{40}$$

and

$$\Delta R_z^{3D} = (4.41\times10^{-7})\sqrt[3]{L_f/(4\gamma\pi^5 d^4)}(at\sigma/h^2)H/(LW) \tag{41}$$

The overall change in resistance ΔR^{3D} in the specimen is equal to the weighted average of ΔR_x^{3D}, ΔR_y^{3D} and ΔR_z^{3D}, i.e.,

$$\Delta R^{3D} = w_x \Delta R_x^{3D} + w_y \Delta R_y^{3D} + w_z \Delta R_z^{3D} \tag{42}$$

where w_x, w_y and w_z are weighting factors that are defined as

$$w_x = L/(L+W+H), \tag{43}$$

$$w_y = W/(L+W+H) \tag{44}$$

and

$$w_z = H/(\mathrm{L+W+H}). \tag{45}$$

Based on our prior experimental work [19,20], d=15 μm, L_f=0.5 cm and γ=0.48 vol.%. Since the maximum value of h is equal to half of the length of a fiber and the amount of crack opening is less than 1 μm [21], h=0.25 cm. Using International Units and substituting these parameters into Eqs. (39)–(42), we have

$$\begin{aligned}\Delta R^{3D} = 1.81\times10^4[&w_x L/(WH) + w_y W/(LH) \\ &+ w_z H/(LW)]at\sigma\end{aligned} \tag{46}$$

From our prior experimental work for the case of uniaxial compression [19], L=5.1 cm, W=5.1 cm and H=3.0 cm. Substituting these values in Eqs. (43)–(46) yields

$$\Delta R^{3D} = 5.14\times10^5 at\sigma. \tag{47}$$

Similarly, from our prior experimental work for the case of uniaxial tension [20], L= 7.0 cm, W=3.0 cm and H=2.0 cm. Substituting these values in Eqs. (43)–(46) yields

$$\Delta R^{3D} = 1.36\times10^6 at\sigma. \tag{48}$$

Substituting into Eqs. (47) and (48) the measured values of stress ó from our prior piezoresistivity experimental work [19,20] and fitting these experimental piezoresistivity data with the model yield the value of at, which is the product of a (half of the length of a crack) and t (the thickness of the crack) and serves as an adjustable parameter in the theory. The average value of at over the range of applied stress for all 3 cycles of the experiment was thus determined to be 50.5 μm^2 and 61.3 μm^2 for uniaxial compression and uniaxial tension respectively.

Table 1 shows different combinations of a and t that correspond to at=50.5 μm^2 and 61.3 μm^2 for the cases of uniaxial compression

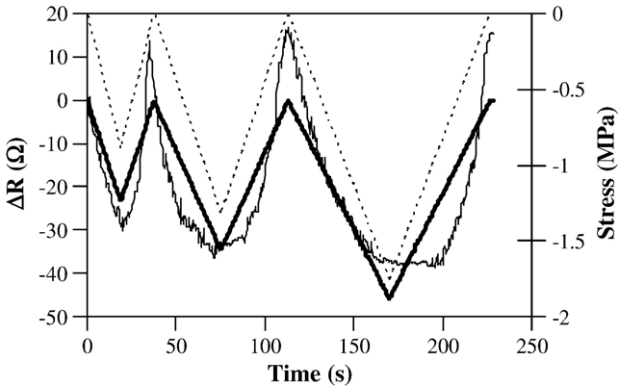

Fig. 7. Curves of measured and calculated values of the change in electrical resistance versus time and of the measured stress versus time under uniaxial compression for at=50.5 μm^2. The measured values are from Ref. 19.

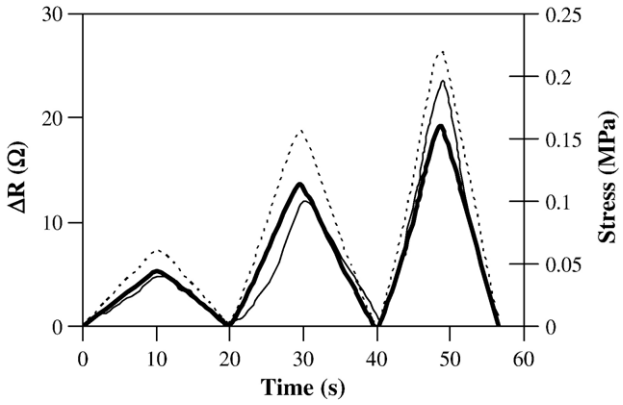

Fig. 8. Curves of measured and calculated values of the change in electrical resistance versus time and of the measured stress versus time under uniaxial tension for at=61.3 μm^2. The measured values are from Ref. 20.

and uniaxial tension. For a given value of at, the larger is t, the smaller is a. As a should be larger than t for a typical crack, the combinations of a and t in Rows 1 to 3 of Table 1 are infeasible. Although a is larger than t in Rows 5 and 6, the value of a is too large, while that of t is too small. The combination of a and t in Row 4 is the most reasonable. Hence, a=50.5 ìm and t=1.0 μm. Table 1 also shows that at a fixed value of t, a is larger for tension than for compression. That a is larger for tension is consistent with the low fracture toughness of cement under tension. By using the a and t values in Row 4, good agreement was obtained between the calculated and experimental values of the change in resistance, as shown in Figs. 7 and 8 for uniaxial compression and uniaxial tension respectively. This agreement supports the model of this paper and furthermore means that most (if not all) of the fibers in a specimen contributes to the piezoresistivity.

This model has also been applied to the piezoresistivity of carbon fiber reinforced cement under flexure. Under flexure, one surface is under tension and the opposite surface is under compression. The surface electrical resistance on each of the tension and compression sides of the beam is measured during flexure [22]. Good agreement between the calculated and measured values of the surface resistances during flexure [23] provides further support of the model presented here.

3. Conclusion

A model of the piezoresistivity in carbon fiber cement is provided, based on the notion that the phenomenon is due to the slight pull-out of crack-bridging fibers during crack opening and the consequent increase in the contact electrical resistivity of the fiber-matrix interface. Good agreement between model and experiment was attained for both tension and compression. Most of the fibers in the specimen contribute to the piezoresistive phenomenon.

Acknowledgement

This work was supported in part by the U.S. National Science Foundation. The technical discussion with Dr. Sirong Zhu of the University at Buffalo is greatly appreciated.

Appendix A. Glossary of symbols

γ	Volume fraction of fibers in the specimen
δ	Distance between the ends of two adjacent fibers (also the thickness of one slice)
ρ_c	Contact electrical resistivity between fiber and matrix
ρ_f	Volume electrical resistivity of a fiber
ρ_m	Volume electrical resistivity of the cement matrix
σ	Tensile stress
θ	Angle between the minor axis and the stress direction
τ	Shear stress applied to a fiber
a	Major axis of an elliptical crack
A	Upper part of the matrix in a unit cell
A_c	Contact area between a fiber and the cement matrix
A_p	Projected area of a crack
A_m	Cross-sectional area of part B of a unit cell
b	Minor axis of an elliptical crack
B	Middle part of the matrix in a unit cell
c	Proportionality constant that relates the resistance change and the shear stress change
C	Lower part of the matrix in a unit cell
d	Fiber diameter
F_c	Force applied on a crack
F_i	Component of F_c along the major axis of a crack
F_j	Component of F_c along the minor axis of a crack
h	Embedded length of a fiber in the cement matrix
H	Height of a parallelepiped measured portion of a specimen
k	Slope of the curve of contact electrical resistivity versus shear stress
L	Length of a parallelepiped measured portion of a specimen
L_f	Fiber length
L_m	Length of part B of a unit cell in the fiber direction
L_p	Projected length of the major axis of a crack
M	Length of a unit cell (cell containing one fiber end)
N	Number of fibers in the measured part of the specimen
N_x	Number of fiber ends in the measured part of the specimen within length L along the x axis
N_y	Number of fiber ends in the measured part of the specimen within width W along the y axis
N_z	Number of fiber ends in the measured part of the specimen within height H along the z axis
Q	Width of a unit cell (cell containing one fiber end)
R	Total resistance of a unit cell in the fiber direction
R_A	Volume resistance of part A of a unit cell
R_B	Volume resistance of part B of a unit cell
R_C	Volume resistance in part C of a unit cell
R_v	Volume resistance of a fiber along the fiber axis
R_i	Contact resistance between a fiber and the cement matrix
R_f	Overall resistance due to a fiber
ΔR^V	Change in resistance of a column in a unit cell
ΔR^{2D}	Change in resistance of a slice in a unit cell
ΔR_x^{3D}	Change in resistance of the measured part of the specimen, if all the fibers are parallel to the x axis

ΔR_y^{3D} Change in resistance of the measured part of the specimen, if all the fibers are parallel to the y axis

ΔR_z^{3D} Change in resistance of the measured part of the specimen, if all the fibers are parallel to the z axis

ΔR^{3D} Total change in resistance of the measured part of the specimen

S Height of a unit cell (cell containing one fiber end)

t Crack width

V_f Volume of an individual fiber

V_s Volume of the measured part of the specimen

V_u Volume of a unit cell

W Width of a parallelepiped measured portion of a specimen

w_x Weighting factor for the contribution to the total change in resistance of the measured part of the specimen for the case in which all the fibers are parallel to the x axis

w_y Weighting factor for the contribution to the total change in resistance of the measured part of the specimen for the case in which all the fibers are parallel to the y axis

w_z Weighting factor for the contribution to the total change in resistance of the measured part of the specimen for the case in which all the fibers are parallel to the z axis

References

[1] P. Chen, D.D.L. Chung, Smart Mater. Struct. 2 (1993) 22–30.
[2] P. Chen, D.D.L. Chung, Compos., Part B Eng. 27B (1996) 11–23.
[3] P. Chen, D.D.L. Chung, J. Am. Ceram. Soc. 78 (3) (1995) 816–818.
[4] D.D.L. Chung, Smart Mater. Struct. 4 (1995) 59–61.
[5] P. Chen, D.D.L. Chung, ACI Mater. J. 93 (4) (1996) 341–350.
[6] X. Fu, D.D.L. Chung, Cem. Concr. Res. 26 (1) (1996) 15–20.
[7] X. Fu, E. Ma, D.D.L. Chung, W.A. Anderson, Cem. Concr. Res. 27 (6) (1997) 845–852.
[8] X. Fu, D.D.L. Chung, Cem. Concr. Res 27 (9) (1997) 1313–1318.
[9] X. Fu, W. Lu, D.D.L. Chung, Carbon 36 (9) (1998) 1337–1345.
[10] Z. Shi, D.D.L. Chung, Cem. Concr. Res. 29 (3) (1999) 435–439.
[11] Q. Mao, B. Zhao, D. Sheng, Z. Li, J. Wuhan U. Tech., Mater. Sci. Ed. 11 (3) (1996) 41–45.
[12] Q. Mao, B. Zhao, D. Shen, Z. Li, Fuhe Cailiao Xuebao/Acta Mater. Compos. Sin. 13 (4) (1996) 8–11.
[13] M. Sun, Q. Mao, Z. Li, J. Wuhan U. Tech., Mater. Sci. Ed. 13 (4) (1998) 58–61.
[14] B. Zhao, Z. Li, D. Wu, J. Wuhan Univ. Tech., Mater. Sci. Ed. 10 (4) (1995) 52–56.
[15] D.D.L. Chung, J. Intell. Mater. Syst. Struct. 13 (9) (2002) 599–609.
[16] X. Fu, D.D.L. Chung, Cem. Concr. Res. 25 (7) (1995) 1391–1396.
[17] P. Chen, D.D.L. Chung, J. Electron. Mater. 24 (1) (1995) 47–51.
[18] S. Wen, D.D.L. Chung, Cem. Concr. Res. 29 (6) (1999) 961–965.
[19] S. Wen, D.D.L. Chung, Cem. Concr. Res. 31 (2) (2001) 297–301.
[20] S. Wen, D.D.L. Chung, Cem. Concr. Res. 30 (8) (2000) 1289–1294.
[21] P. Chen, D.D.L. Chung, Composites 24 (1) (1993) 33–52.
[22] S. Wen, D.D.L. Chung, Carbon 44 (8) (2006) 1496–1502.
[23] Zhu, S. and Chung, D.D.L., J. Mater. Sci., in press.